LEGIBILITY NOTICE

A major purpose of the Technical Information Center is to provide the broadest dissemination possible of information contained in DOE's Research and Development Reports to business, industry, the academic community, and federal, state and local governments.

Although a small portion of this report is not reproducible, it is being made available to expedite the availability of information on the research discussed herein.

1

ORNL/TM-10419

OAK RIDGE NATIONAL LABORATORY

MARTIN MARIETTA

Design and Calibration of a Two-Channel Low-Noise Heterodyne Receiver for Use in a CO_2 Laser Thomson Scattering Alpha Particle Diagnostic

C. A. Bennett
R. K. Richards
D. P. Hutchinson

OPERATED BY
MARTIN MARIETTA ENERGY SYSTEMS, INC.
FOR THE UNITED STATES
DEPARTMENT OF ENERGY

ORNL/TM--10419

DE88 007866

ORNL/TM-10419
Dist. Category UC-20f

Physics Division

DESIGN AND CALIBRATION OF A TWO-CHANNEL LOW-NOISE HETERODYNE RECEIVER FOR USE IN A CO_2 LASER THOMSON SCATTERING ALPHA PARTICLE DIAGNOSTIC

C. A. Bennett,* R. K. Richards, and D. P. Hutchinson

*Department of Physics, University of North Carolina, Asheville, NC 28814

Date Published - March 1988

Prepared by the
OAK RIDGE NATIONAL LABORATORY
Oak Ridge, Tennessee 37831
operated by
MARTIN MARIETTA ENERGY SYSTEMS, INC.
for the
OFFICE OF FUSION ENERGY
U.S. DEPARTMENT OF ENERGY
under Contract No. DE-AC05-84OR21400

TABLE OF CONTENTS

DESIGN AND CALIBRATION OF A TWO-CHANNEL LOW-NOISE HETERODYNE RECEIVER FOR USE IN A CO_2 LASER THOMSON SCATTERING ALPHA PARTICLE DIAGNOSTIC

C. A. Bennett,* R. K. Richards, and D. P. Hutchinson

ABSTRACT

A dual channel low noise heterodyne receiver has been constructed as part of a development effort to build a carbon dioxide laser based Thomson scattering alpha particle diagnostic for a burning plasma experiment. The receiver employs two wide bandwidth (>1 GHz) HgCdTe photovoltaic mixers followed by low noise IF amplifiers. A noise equivalent power of less than 3.0×10^{-20} W/Hz has been demonstrated. Design details and calibration methods are described.

INTRODUCTION

It has been established that heterodyne spectroscopy of Doppler shifted Thomson scattered CO_2 laser radiation can provide a promising method for determining the kinetics of fusion produced alpha particles.[1-3] A crucial component of such a diagnostic is the heterodyne receiver; this system must exhibit low internal noise along with a detection bandwidth large enough to ensure an adequate post detection signal to noise ratio. In what follows, we describe a receiver system utilizing a HgCdTe photovoltaic photomixer with noise and bandwidth capabilities necessary to provide data for alpha particle densities equal to or greater than 10^{11} cm^{-3}.[3] We also describe a method for producing an absolute broadband sensitivity calibration by referencing the output of the receiver to a blackbody standard; this will provide a real time check for photomixer sensitivity changes, system alignment drift, and neutron damage to the optical train.

HETERODYNE DETECTION

The heterodyne signal results from intensity fluctuations as two electromagnetic waves of different frequencies interfere at the surface of a linear power detector. Consider two identically polarized plane electromagnetic waves incident normally on a photomixer, giving a total electric field of

$$E_T = E_1 \cos \omega_1 t + E_2 \cos \omega_2 t \tag{1}$$

Power fluctuations at the intermediate frequency (IF) $\omega_1 - \omega_2$ produce the signal current

$$i_s = \frac{2\eta e}{h\nu} \sqrt{P_1 P_2} \cos (\omega_1 - \omega_2)t \tag{2}$$

where P_1 and P_2 are the powers of the incident electromagnetic waves, $h\nu$ is the incident photon energy, and η is the d.c. quantum efficiency. Amplification of this signal by IF amplifiers and subsequent signal processing give an integrated receiver output proportional to $\langle i_s{}^2 \rangle$ and hence proportional to the product of the incident beam powers. In practice, one of the beams is produced by a local oscillator (LO) with beam power P_{LO}, and the other beam contains the signal power P_s. For a given P_s, the signal is enhanced by increasing P_{LO} until the point where thermal input into the photomixer begins to produce excessive noise. Under ideal circumstances, $P_{LO} \gg P_s$, and the system noise consists mainly of quantum mechanical or shot noise with a contribution due to thermal noise generated within the photomixer and within the IF amplifiers. For a reversed bias photovoltaic photomixer, the noise equivalent power per unit frequency interval (NEP) is:[4]

$$NEP = \frac{h\nu}{\eta}\left\{1 + 2k\,\frac{(T_m + T'_{IF})}{eI_o}\,G_D\left[1 + \left(\frac{f}{f_c}\right)^2\right]\right\}$$

$$= \frac{h\nu}{\eta'} \qquad (3)$$

where k = Boltzman's constant, T_m = photomixer temperature, T'_{IF} = effective input noise temperature of the IF amplifiers, G_D = reverse shunt conductance of the photodiode, I_o = LO induced photocurrent, e = elementary charge, η = d.c. quantum efficiency, η' = heterodyne quantum efficiency, and f_c = 3 dB cutoff frequency of the photodiode. The first term in Eq. (3) represents the shot noise contribution while the second term accounts for thermal noise.

Contributions from the signal power and from the noise power appear at the output of the amplifier; this signal is subsequently rectified, averaged, and amplified to give a d.c. output linearly proportional to the signal power. The post detection signal to noise ratio accounts for this signal averaging, and is given by[5]

$$SNR_{pd} = \frac{P_s}{P_s + P_N}\sqrt{B\tau + 1} \qquad (4)$$

where B = IF bandwidth, τ = signal integration time, P_s = signal power, and P_N = noise power with

$$P_N = (NEP)B \qquad (5)$$

Note that the SNR_{pd} becomes independent of the signal power when $P_s >> P_N$.

SYSTEM DESIGN AND CALIBRATION

Figure 1 shows the optical layout of the two-receiver system. The output of a pulsed CO_2 laser produces the scattered signal. Since it will be necessary to utilize small forward scattering angles,[1,3] a hot cell filled with CO_2 will be used to protect the detectors from stray radiation at the scattering laser frequency.[6] The local oscillator beams are prepared from the attenuated fundamental mode outputs of small waveguide lasers operating at frequencies appropriately shifted from the scattering laser frequency.[1] Two percent beam splitters are used to colinearly combine the LO and signal beams, while the focal lengths of the ZnSe objective lenses are carefully chosen to give an optimum spot size to detector dimension relationship.[7] Three different HgCdTe photodiodes were utilized in this study: a 125-μm-diam detector from Santa Barbara Research Center (SBRC) and two 100-μm-diam detectors from Societe-Anonyme de Telecommunications (SATC). Each detector was equipped with a Dewar capable of maintaining an operating temperature of around 77 K. In the optical train illustrated in Fig. 1, a 50-50 beamsplitter divides the incoming light so that the two detectors share the same signal beam; this would be appropriate for the case where the signal power was large enough to saturate the SNR_{pd}. For smaller signal powers, an additional hot cell could be added.

Figure 2 shows the calibration setup. The chopper wheel is covered with an absorbing layer of high emissivity material and is maintained at

ORNL-DWG 88-7355

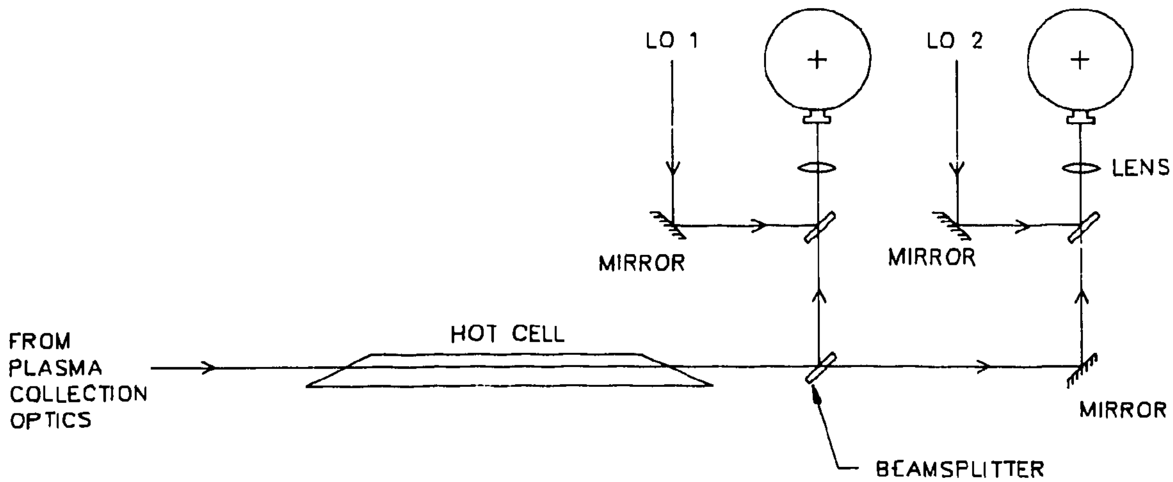

Fig. 1. Optical layout of the two-receiver system.

ORNL-DWG 88-7356

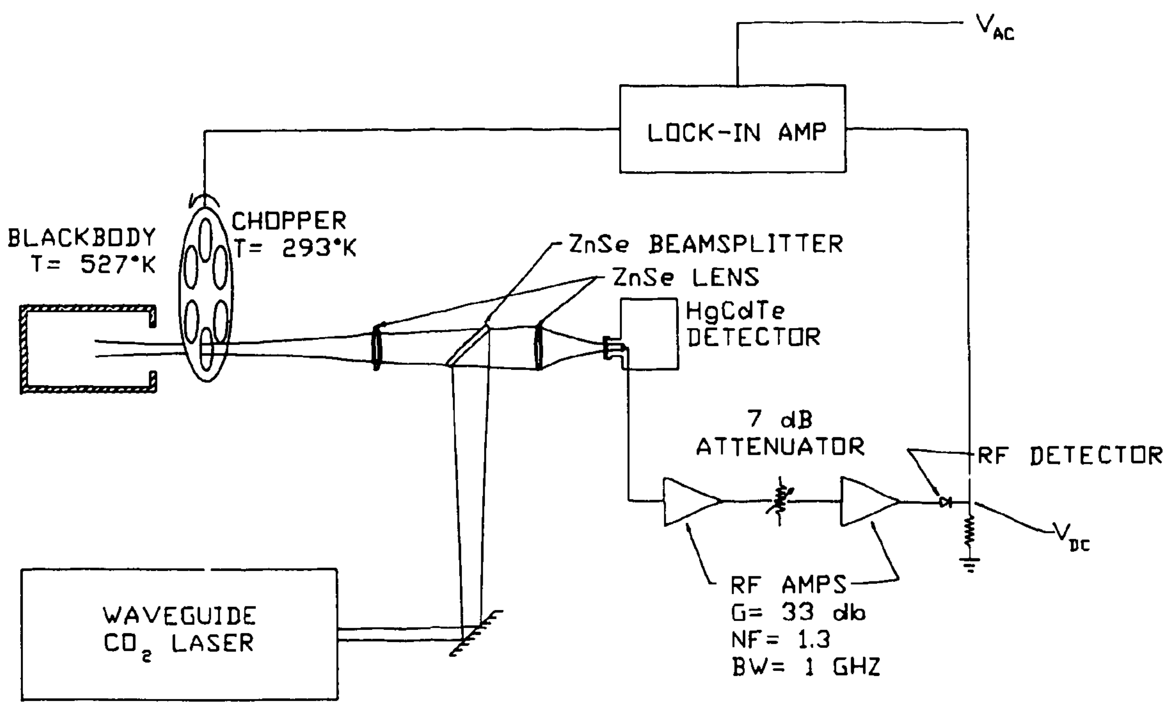

Fig. 2. Calibration setup.

room temperature. A variable temperature blackbody source produces the signal power. An additional ZnSe lens forms a reverse projection of the LO beam which fits entirely within the aperture of the blackbody source.[8] Amplification is achieved with dual Miteq AM-3A-00110 amplifiers equipped with an attenuator between the amplifier stages to prevent saturation of the second amplification stage. Each amplifier has 33 dB of gain, a noise figure of 1.3 and a 1-GHz bandwidth. An RF diode rectifies the amplified signal and this voltage is measured with a digital voltmeter. The a.c. component of the rectified signal is analyzed by a lock-in amplifier which is referenced by the chopper.

Figure 3 illustrates the signal at the input of the lock-in amplifier. The rectified IF signal is modulated beneath an approximately square wave envelope oscillating between V_1 and V_2 at the chopping frequency. These voltages are given by

$$V_1 = C[P_N BA + P_R\ (2B)\ A]$$
$$V_2 = C[P_N BA + P_B\ (2B)\ A] \qquad (6)$$

where A = amplification, P_R = blackbody power signal per unit frequency interval from the chopper wheel, P_B = blackbody power signal per unit frequency interval from the elevated temperature source, C = constant, and B = IF amplifier bandwidth. Note that the heterodyne signal is generated over a double-side band whereas the noise is generated within a single bandwidth only [see Eq. (5)]. Solving for P_N in terms of V_1 and V_2 and then recasting in terms of the measured voltages V_{ac} and V_{dc}, we obtain

ORNL-DWG 88-7357

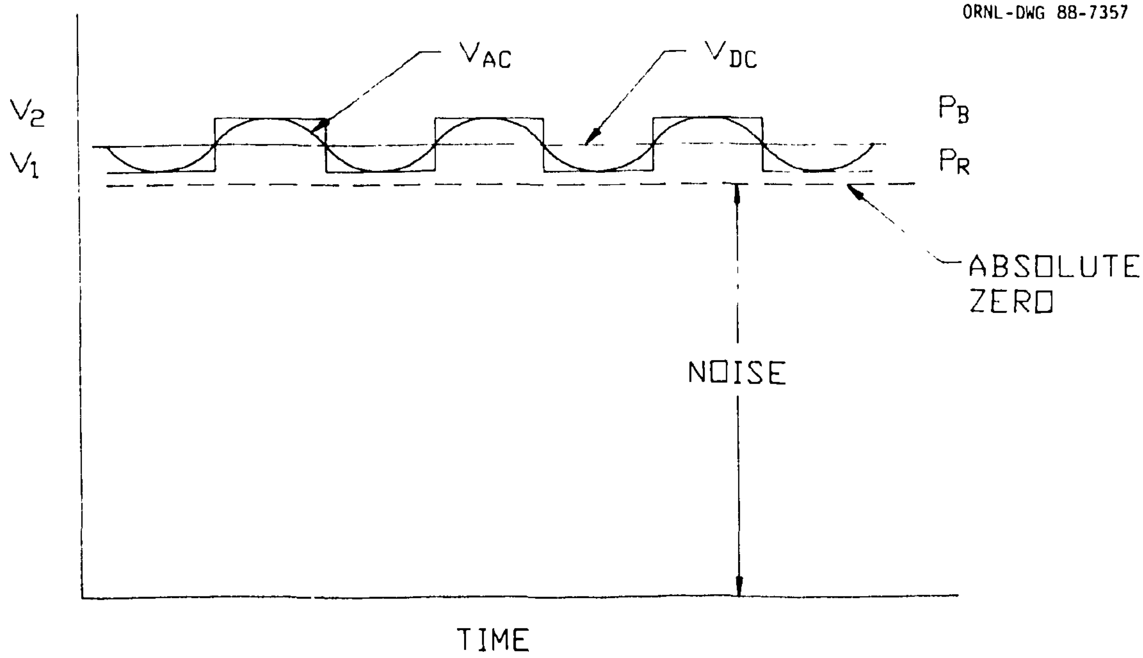

Fig. 3. Representation of the signal voltages at the input of the lock-in amplifier.

$$NEP = 2 \ \ V_{dc}/\alpha \ V_{ac} - \frac{1}{2} \ (P_B - P_R) - 2P_R \qquad (7)$$

where α accounts for the fact that the lock-in amplifier measures only the fundamental component of the modulating envelope; our chopper wheel aperture and LO beam shape gave $\alpha = 2.26$. The blackbody signals are calculated according to[8]

$$P = \frac{h\nu}{e^{h\nu/kT} - 1} \qquad (8)$$

Under broadband conditions, the observed voltage levels consisted of an a.c. component of around 0.5 mv and a d.c. component of about 10 to 20 mv; these voltages were conveniently monitored on an oscilloscope placed across the RF diode as the system alignment and LO power were adjusted for optimum receiver performance. The system noise levels and quantum efficiencies were easily optimized to the values indicated in Table 1.

Table 1. Optimum performance for the three photomixers investigated

Detector	NEP	Heterodyne Quantum Efficiency
SBRC	5.0×10^{-20}	38%
SATC1	2.7×10^{-20}	70%
SATC2	4.7×10^{-20}	40%

It should be noted that this method measures the integrated sensitivity of the entire receiver system. An optical layout which would allow the field of view of the receiver to be filled with a blackbody source upon demand will result in a system with the capability to be accurately calibrated at regular intervals. This capability will be important for the above mentioned alpha particle experiment since the neutron flux may degrade the transmission of the optical elements and since vacuum vessel excursions may perturb the system alignment. By using a spectrum analyzer as a tunable filter, the frequency response of the system could be determined. Figure 4 shows the NEP vs IF frequency for the SBRC and the SATC1 photomixers when the bandpass of the spectrum analyzer was set to 3 MHz. The lowest frequency data were fairly close to the centerburst of the spectrum analyzer while the structure in the SATC data was probably due to a VSWR resonance.

ORNL-DWG 87C-13564

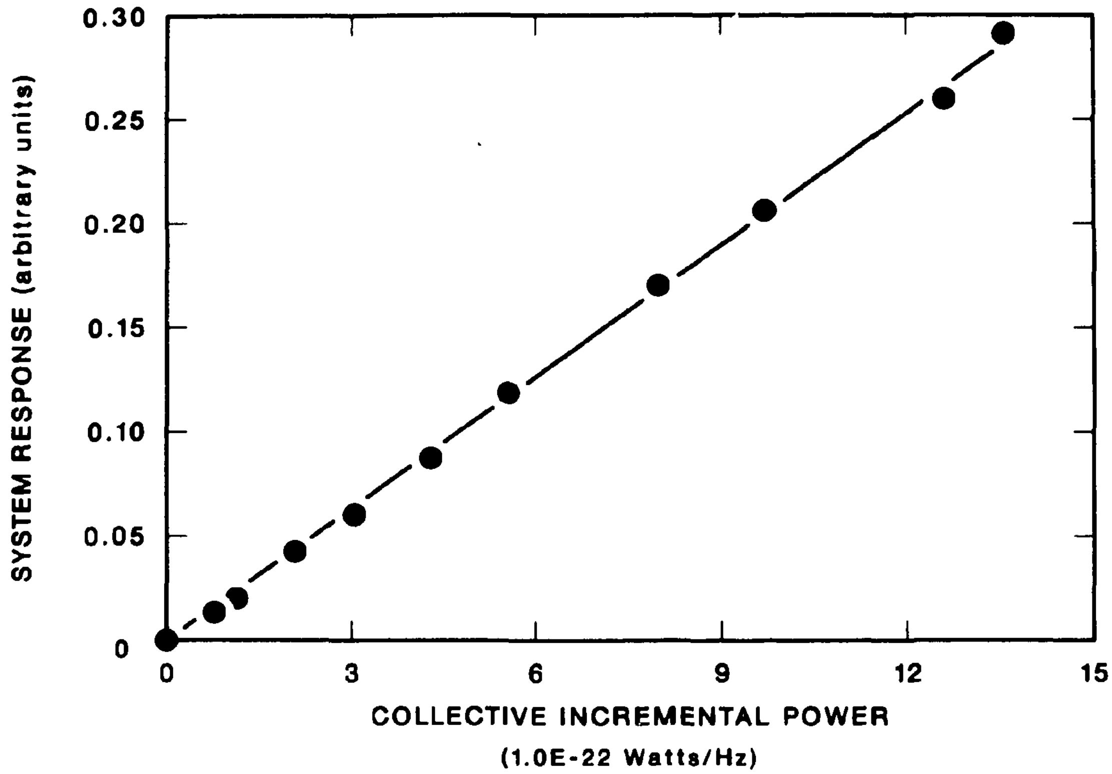

Fig. 4. System NEP vs IF frequency.

The linearity of the receiver to changes in signal power is illustrated in Fig. 5. These data represent the change in system response as the temperature of the blackbody was changed between 45°C and 254°C. The signal power levels were calculated according to Eq. (8).

CONCLUSIONS

A low noise, large bandwidth two channel heterodyne receiver has been developed with sensitivity more than adequate for a proposed CO_2 laser based Thomson scattering alpha particle diagnostic. An absolute broadband calibration procedure has been designed which references the

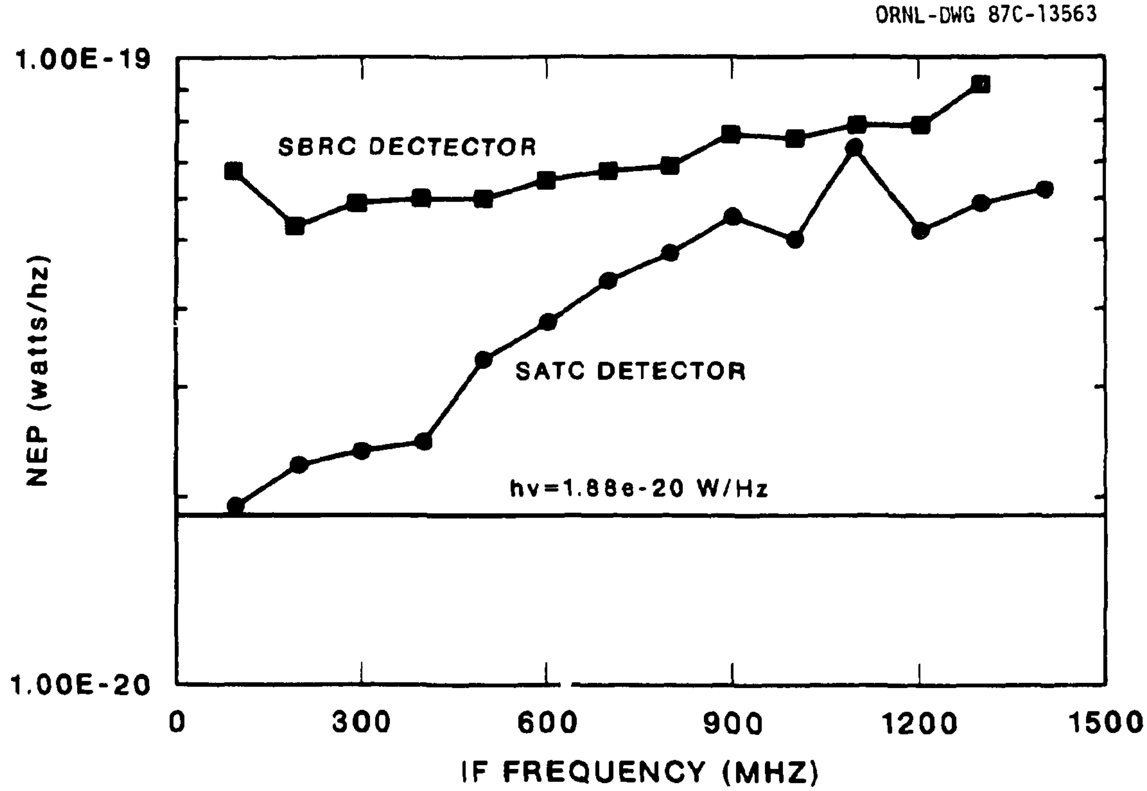

Fig. 5. System linearity as a function of changes in signal power.

system noise to the output of a blackbody standard. This calibration procedure can be easily integrated into the alpha particle experiment so that system sensitivity checks can routinely be made.

REFERENCES

*Department of Physics, University of North Carolina at Asheville, Asheville, NC 28814.

1. D. P. Hutchinson, K. L. Vander Sluis, J. Sheffield, and D. J. Sigmar, Feasibility of Alpha Particle Measurement by CO_2 Laser Scattering, ORNL/TM-9090, Martin Marietta Energy Systems, Inc., Oak Ridge Natl. Lab., December 1984.

2. L. Vahala, G. Vahala, and D. J. Sigmar, "Effects of Alpha Particles on the Scattering Function in CO_2 Laser Scattering," Nucl. Fusion 26, 51 (1986).

3. R. K. Richards, K. L. Vander Sluis, and D. P. Hutchinson, Feasibility of Alpha Particle Measurement in a Magnetically Confined Plasma by CO_2 Laser Thomson Scattering, ORNL/TM-10363, Martin Marietta Energy Systems, Inc., Oak Ridge Natl. Lab., March 1987.

4. B. J. Peyton, A. J. DiNardo, G. M. Kanishak, F. R. Arams, R. M. Lange, and E. W. Sard, "High Sensitivity Receiver for Infrared Laser Communications," IEEE J. Quantum Electron. QE-8, 252 (1972).

5. E. Holzhauer and J. H. Massig, "An Analysis of Optical Mixing in Plasma Scattering Experiments," Plasma Phys. 20, 867 (1978).

6. N. Bretz and G. Taylor, Design and Performance Study of an Extreme Forward CO_2 Laser Scattering Measurement of TI on TFTR, Princeton Plasma Physics Report #47, 1982.

7. T. Takenaka, K. Tanaka, and O. Fukumitsu, "Signal to Noise Ratio in Optical Heterodyne Detection for Gaussian Fields," Appl. Opt. 17, 3466 (1978).

8. A. E. Siegman, "The Antenna Properties of Optical Heterodyne Receivers," Proc. IEEE 54, 1350 (1966).

INTERNAL DISTRIBUTION

1. J. B. Ball
2. W. H. Casson
3. H. T. Hunter
4-8. D. P. Hutchinson
9. C. H. Ma
10. F. M. Ownby
11. R. A. Phaneuf
12-16. R. K. Richards
17. J. Sheffield
18. K. L. Vander Sluis
19. Fusion Energy Division Library
20. Central Research Library
21. Document Reference Section
22-23. Laboratory Records
24. Laboratory Records, RC
25. ORNL Patent Section

EXTERNAL DISTRIBUTION

26. Office of the Assistant Manager for Energy Research and Development, Department of Energy, Oak Ridge Operations, Box E, Oak Ridge, TN 37831
27-31. C. A. Bennett, Dept. of Physics, Univ. of North Carolina, Asheville, NC 28814
32. Bibliothek, Institut fur Plasmaphysik, KFA, Postfach 1913, D-5170 Julich, Federal Republic of Germany
33. Bibliothek, Max-Planck Institut fur Plasmaphysik, D-8046 Garching bei Munchen, Federal Republic of Germany
34. Bibliotheque, Centre de Recherches en Physique des Plasmas, 21 Avenue des Bains, 1007 Lausanne, Switzerland
35. Bibliotheque, Service due Confinement des Plasma, CEA, B.P. 6, 92 Fontenay-aux-Roses (Seine), France
36. N. L. Bretz, Princeton Plasma Physics Laboratory, P.O. Box 451, Princeton, NJ 08544
37. J. D. Callen, Department of Nuclear Engineering, University of Wisconsin, Madison, WI 53706
38. R. W. Conn, Department of Chemical, Nuclear, and Thermal Engineering, University of California, Los Angeles, CA 90024
39. D. H. Crandall, ER-542 GTN, Office of Fusion Energy, U.S. Department of Energy, Washington, DC 20545
40. S. O. Dean, Fusion Energy Development, Science Applications, Inc., 2 Professional Drive, Gaithersburg, MD 20760
41. Documentation S.I.G.N., Department de la Physique du Plasma et de la Fusion Controlee, Centre d'Etudes Nucleaires, B.P. No. 85, Centre du Tri, 38041 Cedex, Grenoble, France
42. G. A. Eliseev, I. V. Kurchatov Institute of Atomic Energy, P.O. Box 3402, 123182 Moscow, U.S.S.R.
43. D. Evans, Culham Laboratory, Abingdon, Oxon. OX14 3DB, United Kingdom
44. M. Forrest, JET, Culham Laboratory, Abingdon, Oxon. OX14 3DB, United Kingdom

45. H. K. Forsen, Bechtel Group, Inc., Research Engineering, P.O. Box 3965, San Francisco, CA 94105
46. J. R. Gilleland, GA Technologies, Inc., Fusion and Advanced Technology, P.O. Box 85608, San Diego, CA 92138
47. V. A. Glukhikh, Scientific-Research Institute of Electro-Physical Apparatus, 188631 Leningrad, U.S.S.R.
48. R. W. Gould, Department of Applied Physics, California Institute of Technology, Pasadena, CA 91125
49. C. Gowers, JET, Culham Laboratory, Abingdon, Oxon. OX14 3DB, United Kingdom
50. R. A. Gross, Plasma Research Laboratory, Columbia University, New York, NY 10027
51. F. C. Jahoda, Los Alamos Scientific Laboratory, University of California, P.O. Box 1663, Los Alamos, NM 87545
52. Library, Culham Laboratory, UKAEA, Abingdon, Oxfordshire, OX14 3DB, England
53. Library, FOM Institut voor Plasma-Fysica, Rijnhuizen, Jutphaas, The Netherlands
54. Library, Institute of Physics, Academia Sinica, Beijing, People's Republic of China
55. Library, Institute of Plasma Physics, Nagoya University, Nagoya 464, Japan
56. Library, International Centre for Theoretical Physics, Trieste, Italy
57. Library, Laboratorio Gas Ionizzati, Frascati, Italy
58. Library, Plasma Physics Laboratory, Kyoto University, Gokasho Uji, Kyoto, Japan
59. N. C. Luhmann, 7702 Boelter Hall, Electrical Engineering Department, School of Engineering and Applied Science, 405 Hilgard Ave., University of California, Los Angeles, CA 90024
60. K. McCormick, Max-Planck Institut fuer Plasmaphysik, 8046 Garching bie Munchen, West Germany
61. D. M. Meade, Plasma Physics Laboratory, Princeton University, P.O. Box 451, Princeton, NJ 08544
62. R. R. Patty, Dept. of Physics, North Carolina State Univ., Raleigh, NC 27650
63. Plasma Research Laboratory, Australian National University, P.O. Box 4, Canberra, A.C.T. 2000, Australia
64. D. H. Priester, ER-542 GTN, Office of Fusion Energy, U.S. Department of Energy, Washington, DC 20545
65. P. J. Reardon, Brookhaven National Laboratory, Upton, NY 11973
66. D. D. Ryutov, Institute of Nuclear Physics, Siberian Branch of the Academy of Sciences of the U.S.S.R., Sovetskaya St. 5, 630090 Novosibirsk, U.S.S.R.
67. I. Spighel, Lebedev Physical Institute, Leninsky Prospect 53, 117924 Moscow, U.S.S.R.
68. W. M. Stacey, Jr., School of Nuclear Engineering, Georgia Institute of Technology, Atlanta, GA 30332
69. D. Steiner, Rensselaer Polytechnic Institute, Troy, NY 12181

70. J. D. Strachan, Princeton Plasma Physics Laboratory, P.O. Box 451, Princeton, NJ 08544
71. Thermonuclear Library, Japan Atomic Energy Research Institute, Tokai, Naka, Ibaraki, Japan
72. V. T. Tolok, Kharkov Physical-Technical Institute, Academical St. 1, 310108 Kharkov, U.S.S.R.
73. R. Varma, Physical Research Laboratory, Navrangpura, Ahmedabad, India
74. M. A. Walker, 199 Warren St. NE, Atlanta, GA 30317
75. M. Yamanaka, Dept. of Applied Physics, Osaka University, Yamada-kami, Suita, Osaka 565, Japan
76. K. M. Young, Princeton Plasma Physics Laboratory, P.O. Box 451, Princeton, NJ 08544
77. S. Zweben, Princeton Plasma Physics Laboratory, P.O. Box 451, Princeton, NJ 08544

78-203. Given distribution as shown in TIC-4500 under UC-20f MFE-Experimental Plasma Physics